

Kinematic and Dynamic Modeling of the MAHI Exo-II

Nathan Dunkelberger, Craig G. McDonald

January 2020

1 Introduction

The MAHI Exo-II, shown in Figure 1, is a robotic exoskeleton designed for the rehabilitation of the elbow and wrist joints. It features serially connected joints for elbow flexion/extension (E-Flx/Ext) and forearm pronation/supination (F-Pro/Sup), and a parallel revolute-prismatic-spherical mechanism that achieves wrist flexion/extension (W-Flx/Ext) and wrist radial/ulnar deviation (W-Rad/Uln).

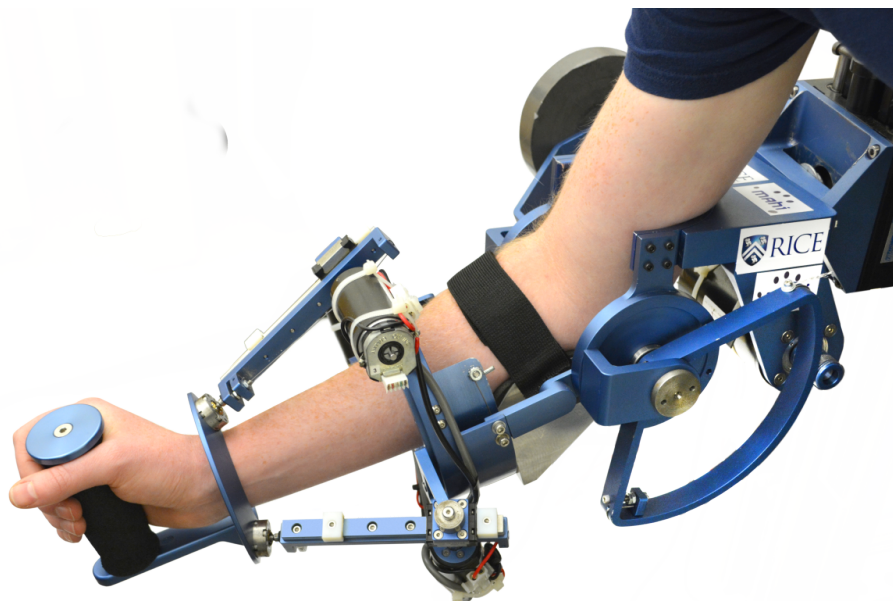


Figure 1: MAHI Exo-II as worn by a user.

Several iterations of wrist exoskeleton design preceded the MAHI Exo-II. The original MAHI exoskeleton design was presented by Gupta and O'Malley [3], along with thorough discussion of the specific design considerations for the device. It is composed of a revolute joint at the forearm for pronation and supination, and a 3-RPS (revolute-prismatic-spherical) serial-in-parallel wrist. The device was then redesigned [5] to address limitations of the original version, and this new design was called the *RiceWrist*. Details of the design, kinematics, and task space control of the wrist platform, which corresponds to anatomical joint space control of the human wrist, can be found in [4].

The most current design iteration by Pehlivan *et al.* [6] includes another serial revolute joint at the base of the *RiceWrist* aligned with the elbow. French *et al.* performed a series of system

identification tasks characterizing the MAHI Exo-II [1], some results of which are listed in Tables 1,2, and 4. (Range of motion is abbreviated as ROM. Bandwidth is abbreviated as BW.)

The MAHI Exo-II is equipped with high-resolution optical encoders at each of the motors, from which we can extract position and velocity of all degrees of freedom. Commanded currents to the actuators can also be used to estimate the torque delivered to the human joints by the robot, though static friction in the robot joints and misalignment between the human and exoskeleton can be significant sources of error in this estimate.

The height and shoulder abduction angle of the MAHI-Exo II can be adjusted and locked to keep both shoulders at equal heights and to keep the shoulder of the user’s active arm in the scapular plane (30° from the frontal plane) for maximal comfort. The wrist handle location can be positioned and locked to provide a maximum range of motion while the user holds it in a natural grip. The MAHI Exo-II is also equipped with an adjustable counterweight for passive gravity compensation of the elbow joint. The exoskeleton can easily be configured for use with the left or right arm, and the user can be strapped into padded cuffs at the upper forearm and upper arm. All of these passive joints can be considered additional degrees of freedom of the robot, which can be useful to define within the kinematic model—especially when considering a connected skeletal model, as in OpenSim.

Table 1: MAHI Exo-II ROM and Torque Output [1]

| Joint | ROM (deg) | Torque (N m) |
|--------------|---------------------|------------------------|
| E-Flx/Ext | 90 | 7.35 |
| F-Pro/Sup | 180 | 2.75 |
| W-Flx/Ext | 65 | 1.45 |
| W-Rad/Uln | 63 | 1.45 |

Table 2: MAHI Exo-II Dynamic Model Parameter Estimation [1]

| Joint | Static Friction (N m) | Inertia (kg m ²) | Viscous Friction (N M s/rad) |
|--------------|---------------------------------|--|--|
| E-Flx/Ext | 0.9491 | 0.2713 | 0.1215 |
| F-Pro/Sup | 0.139 | 0.0257 | 0.0167 |
| W-Flx/Ext | 0.109 | 0.002 | 0.0283 |
| W-Rad/Uln | 0.112 | 0.0033 | 0.0225 |

2 Kinematics

The MAHI Exo-II can be conveniently divided into its proximal, rotary degrees of freedom (DoFs), aligned with the elbow and forearm, and its distal degrees of freedom articulating the wrists. The proximal joints are in a serial RR configuration, while the distal joints compose the revolute-prismatic-serial (RPS) mechanism with 3 independent DoFs.

The kinematics presented here do not strictly follow the Denavit-Hartenburg (DH) convention but instead focus on compatibility with kinematic descriptions used in certain software (e.g. OpenSim),

Table 3: MAHI Exo-II Closed-loop Control [1]

| Joint | Pos. BW (Hz) |
|--------------|-------------------------|
| E-Flx/Ext | 2.8 |
| F-Pro/Sup | 4.2 |
| W-Flx/Ext | 13.3 |
| W-Rad/Uln | 10.6 |

compactness of representation, and handling the complexity of the RPS parallel mechanism. See Table 5 for a list of the values used for the kinematic parameters described in this section.

The following table shows the conventions for angles on the MEII

Table 4: MAHI Exo-II Closed-loop Control [1]

| Joint | -Extreme (value) | +Extreme (value) |
|--------------|----------------------------------|-----------------------------------|
| E-Flx/Ext | Full Extension (-90°) | Flexed 90° (0°) |
| F-Pro/Sup | Supination (-90°) | Pronation ($+90^\circ$) |
| W-Flx/Ext | Extension ($-30^\circ?$) | Flexion ($+30^\circ?$) |
| W-Rad/Uln | Ulnar Deviation ($-30^\circ?$) | Radial Deviation ($+30^\circ?$) |

2.1 Proximal Serial Joints

The following transformation matrices determine the kinematics of the proximal part of the MAHI Exo-II, Figure 2. The kinematic chain they describe is all serially connected.

The first transformation matrix, 0_1T , shows the placement of the MAHI Exo-II, where q_2 and q_3 are the robot base x and z locations respectively, and q_1 is the rotation about the y axis. This places the origin of this coordinate frame at the bottom of the robot support structure, relative to some world Frame 0 that can be thought of as being attached to the user, their seat, or any other reference point.

$${}^0_1T = \begin{bmatrix} c_1 & 0 & -s_1 & c_1q_2 + s_1q_3 \\ 0 & 1 & 0 & -a_0 \\ s_1 & 0 & c_1 & c_1q_3 - s_1q_2 \\ 0 & 0 & 0 & 1 \end{bmatrix}$$

The second transformation matrix, 1_2T , represents the vertical translation of the slide on the robot support structure by general coordinate q_4 .

$${}^1_2T = \begin{bmatrix} 1 & 0 & 0 & 0 \\ 0 & 1 & 0 & q_4 \\ 0 & 0 & 1 & 0 \\ 0 & 0 & 0 & 1 \end{bmatrix}$$

The third transformation matrix, 2_3T , represents the rotation of the exoskeleton with respect to the mounting block that it connects to, and it is associated with shoulder abduction/adduction. This coordinate, q_5 , is changed by loosening the the nut which connects the exoskeleton to the mounting

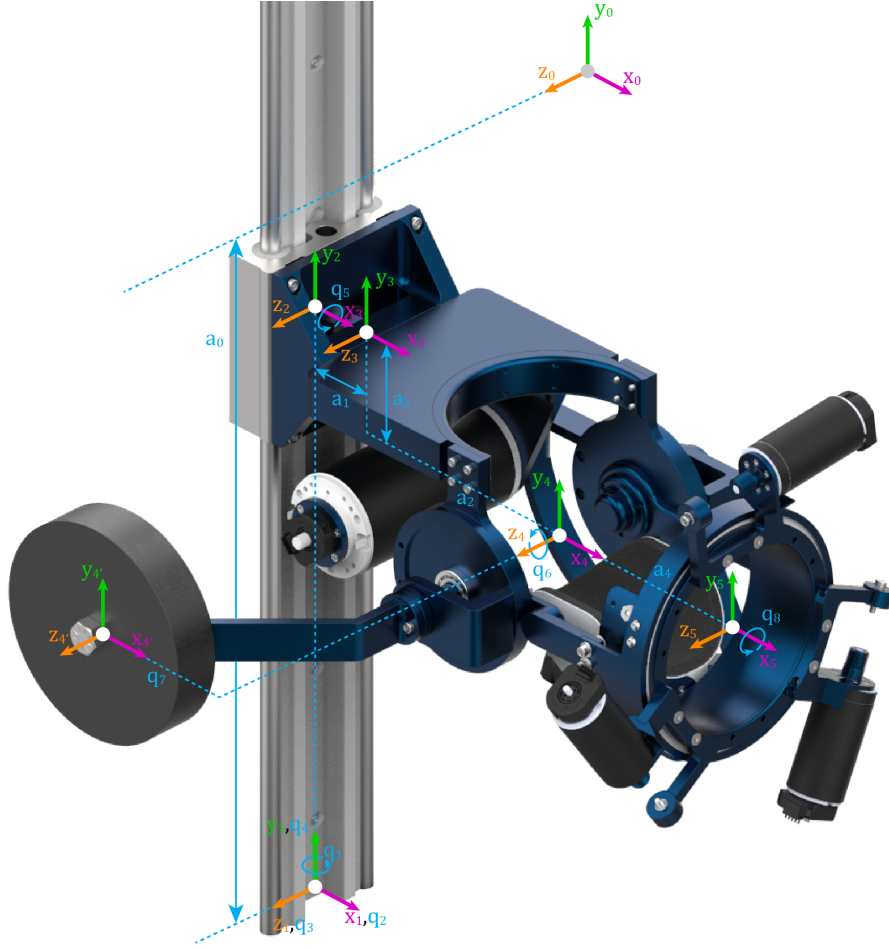


Figure 2: Coordinate frames and parameters shown from the world frame to the forearm.

block and tightening it when it is at its appropriate subject-specific location. The dimension d_5 represents the distance between the center of the bearing sliders on the linear rail and the closest face of the exoskeleton that rotates with q_5 .

$${}^2_3T = \begin{bmatrix} 1 & 0 & 0 & d_1 \\ 0 & c_5 & -s_5 & 0 \\ 0 & s_5 & c_5 & 0 \\ 0 & 0 & 0 & 1 \end{bmatrix}$$

The fourth transformation matrix, 3_4T , represents the rotation of the elbow with respect to the previous portion of the exoskeleton. The elbow rotation is represented by general coordinate q_6 along the z axis. Dimensions a_2 and a_3 represent the distances between O_3 and O_4 in directions \vec{x}_3 and $-\vec{y}_3$ respectively.

$${}^3_4T = \begin{bmatrix} c_6 & -s_6 & 0 & a_2 \\ s_6 & c_6 & 0 & -a_3 \\ 0 & 0 & 1 & 0 \\ 0 & 0 & 0 & 1 \end{bmatrix}$$

The transformation matrix, 4_4T , represents the placement of the counterweight on the exoskeleton. The counterweight translation is represented by general coordinate q_7 along the \vec{x}_4 axis. Dimensions a_{41} and a_{42} represent the distances between O_4 and $O_{4'}$ in directions $-\vec{x}_4$ and \vec{z}_4 respectively.

$${}^4_4T = \begin{bmatrix} 1 & 0 & 0 & -a_{41} - q_7 \\ 0 & 1 & 0 & 0 \\ 0 & 0 & 1 & a_{42} \\ 0 & 0 & 0 & 1 \end{bmatrix}$$

The transformation matrix 4_5T represents the rotation of the forearm using general coordinate q_8 . The dimension a_4 represents the distance between the elbow rotation mechanism and the forearm rotation mechanism in the \vec{x}_4 direction.

$${}^4_5T = \begin{bmatrix} 1 & 0 & 0 & a_4 \\ 0 & c_8 & -s_8 & 0 \\ 0 & s_8 & c_8 & 0 \\ 0 & 0 & 0 & 1 \end{bmatrix}$$

The forearm cuff that serves as a physical interface between the exoskeleton and the user is attached to Frame 5 of the kinematic model.

2.2 Distal RPS Mechanism

This section describes the kinematics of the distal portion of the robot, including 3-DoF revolute-prismatic-serial (RPS) mechanism, Figure 3. It is a parallel mechanism that enables the desired anatomical rotations of wrist flexion-extension and wrist radial-ulnar deviation to be performed with actuators that are further from the anatomical joints, reducing overall weight in that area. There is also a third degree of freedom that allows for exoskeleton alignment with different arm sizes.

The kinematic solution for the RPS mechanism arises from an iterative method for solving closed-chain mechanisms explained in [2]. The first step is to define the constraints that govern this system. There are 12 generalized coordinates that can fully describe the positions and orientations of the rigid bodies, given the inherent constraints of the single-DoF revolute and prismatic joints. Each of the 3 linear rails is able to rotate in 1 dimension and translate in 1 dimension ($3 \times 2 = 6$ DoFs) and the wrist ring is able to rotate and translate in 3 dimensions (6 DoFs). We will represent the rotational DoF of each of the rails as $\theta_i, i \in [1, 2, 3]$, and each translation DoF (occurring serially after rotation) as $l_i, i \in [1, 2, 3]$. The location of the center of the wrist wring is defined by coordinates $[x_c, y_c, z_c]$, and the orientation is defined by Euler rotations of α about the y -axis, β about the z -axis, and γ about the x -axis with respect to coordinate Frame 5.

In this system, there are 9 constraints that must be met in order for the system to be kinematically correct. Those constraints are defined by three paths that begin at the origin of coordinate Frame 5, travel to the forearm ring, along the linear rail to the wrist ring, to the center of the wrist ring, and back to the origin of coordinate Frame 5. That path is described by equation 1.

$$\vec{\phi}_i = {}^5\vec{r}_i + {}^5\vec{l}_i - {}^5R_{13}{}^{13}\vec{b}_i - {}^5\vec{O}_{13} = \vec{0} \quad (1)$$

Each portion of the equation is specified below. ${}^5\vec{r}_i$ specifies the location of R_i represented in coordinate Frame 5 as specified in Figure 4.

$${}^5r_1 = \begin{bmatrix} 0 \\ R_c\alpha_5 - a_{56}s\alpha_5 \\ R_c\alpha_5 + a_{56}s\alpha_5 \end{bmatrix}$$

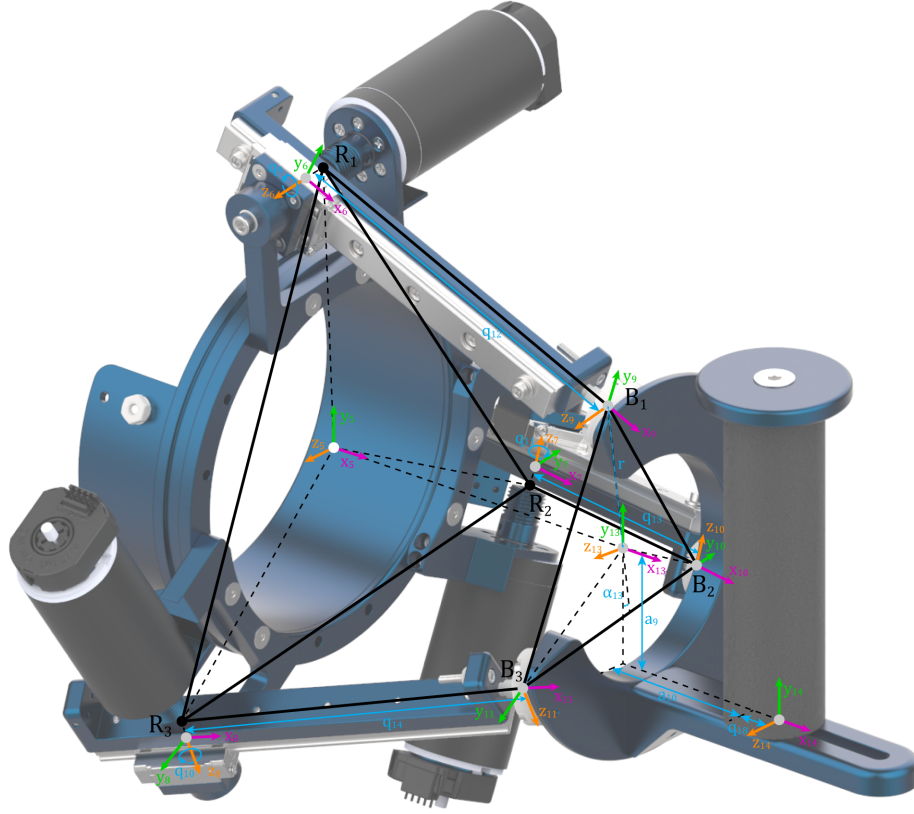


Figure 3: Definitions of coordinate frames and parameters for the RPS mechanism.

$${}^5r_2 = \begin{bmatrix} 0 \\ Rca'_5 - a_{56}s\alpha'_5 \\ Rca'_5 + a_{56}s\alpha'_5 \end{bmatrix}$$

$${}^5r_3 = \begin{bmatrix} 0 \\ Rca''_5 - a_{56}s\alpha''_5 \\ Rca''_5 + a_{56}s\alpha''_5 \end{bmatrix}$$

${}^5\vec{l}_i$ specifies the vector from R_i to B_i represented in coordinate Frame 5 as specified in Figure 4.

$${}^5\vec{l}_1 = \begin{bmatrix} l_1 s\theta_1 \\ -l_1 c\alpha_5 c\theta_1 \\ -l_1 c\alpha_5 s\theta_1 \end{bmatrix}$$

$${}^5\vec{l}_2 = \begin{bmatrix} l_2 s\theta_2 \\ -l_2 c\alpha'_5 c\theta_2 \\ -l_2 c\alpha_5 s\theta_2 \end{bmatrix}$$

$${}^5\vec{l}_3 = \begin{bmatrix} l_3 s\theta_3 \\ -l_3 c\alpha''_5 c\theta_3 \\ -l_3 c\alpha_5 s\theta_3 \end{bmatrix}$$

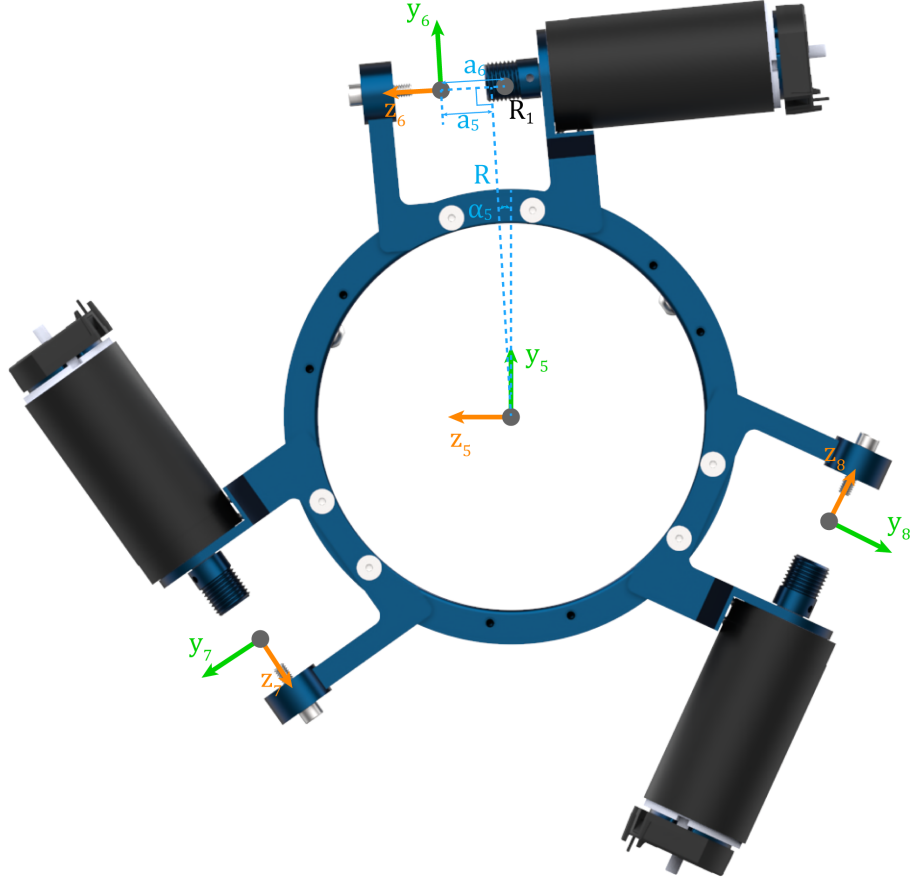


Figure 4: Definitions of coordinate frames and parameters for the forearm ring of the RPS mechanism.

${}^5\vec{b}_i$ specifies the vector from the origin of coordinate Frame 13 to b_i represented in coordinate Frame 13 as specified in Figure 4.

$${}^{13}\vec{b}_1 = \begin{bmatrix} 0 \\ r\alpha_{13} \\ r\sigma_{13} \end{bmatrix}$$

$${}^{13}\vec{b}_2 = \begin{bmatrix} 0 \\ r\alpha'_{13} \\ r\sigma_{13} \end{bmatrix}$$

$${}^{13}\vec{b}_3 = \begin{bmatrix} 0 \\ r\alpha''_{13} \\ r\sigma_{13} \end{bmatrix}$$

${}^5\mathcal{O}_{13}$ specifies the vector from the origin of coordinate Frame 5 (the center of the forearm ring) to the origin of coordinate Frame 13 (the center of the wrist ring) represented in coordinate Frame 5.

$${}^5\vec{\mathcal{O}}_{13} = [x_c \quad y_c \quad z_c]^\top \quad (2)$$

${}^5R_{13}$ specifies the Euler angle rotations from coordinate Frame 5 to the coordinate Frame 13, which is aligned with the *handle* parallel to \bar{y}_{13} . (\bar{y}_{13} is not pointing to B_1 .)

$${}^5R_{13} = R_Y(\alpha)R_Z(\beta)R_X(\gamma) \quad (3)$$

Based on these equations, there are 12 kinematic variables to be found, defined as:

Table 5: Kinematic Parameter Values

| Parameter | Value | Units |
|-----------------|--------------------------------|-------|
| a_0 | 0.5 | m |
| a_1 | 0.0604774 | m |
| a_2 | 0.13335 | m |
| a_3 | 0.0762 | m |
| a_4 | 0.159385 | m |
| a_5 | 0.0268986 | m |
| a_6 | 0.027282 | m |
| R | 0.1044956 | m |
| r | 0.052881745 | m |
| α_5 | 0.094516665 | rad |
| α_{12} | $\frac{20\pi}{180}$ | rad |
| α_{13} | $\frac{5\pi}{180}$ | rad |
| a_{56} | $a_5 - a_6$ | m |
| α'_5 | $\alpha_5 - \frac{2\pi}{3}$ | rad |
| α''_5 | $\alpha_5 + \frac{2\pi}{3}$ | rad |
| α'_{13} | $\alpha_{13} - \frac{2\pi}{3}$ | rad |
| α''_{13} | $\alpha_{13} + \frac{2\pi}{3}$ | rad |
| a_7 | 0.018086622 | m |
| a_8 | 0.049692586 | m |
| a_9 | 0.0381 | m |
| a_{10} | 0.062809158 | m |
| a_{41} | 0.1143 | m |
| a_{42} | 0.24837205 | m |

$$q' = \left[\theta_1 \quad \theta_2 \quad \theta_3 \quad l_1 \quad l_2 \quad l_3 \quad \alpha \quad \beta \quad \gamma \quad x_c \quad y_c \quad z_c \right]^T \quad (4)$$

The 3-D constraint equations for the 3 closed paths of the mechanism are now arranged into a single column vector:

$$\phi(q') = \left[\phi_1^T \quad \phi_2^T \quad \phi_3^T \right]^T \in \mathbb{R}^{9 \times 1} \quad (5)$$

Now, we must choose which variables are to be controlled or specified independently, and the remaining 9 variables will be dependent on them. To do this mathematically, we define an indexing function $\alpha(\cdot)$, which takes as input the full variable set and returns the three selected independent variables. In our case, this can just be accomplished by multiplying our vector of kinematics variables, q' (12×1) by a 12×12 with three 1s on the diagonal corresponding to the chosen independent variables and 0s for all other elements.

$$q^* = \alpha(q') \quad (6)$$

At this point it is helpful to remember the dimensions of the variables we are working with.

$$q' \in \mathbb{R}^{12}, q^* \in \mathbb{R}^3 \quad (7)$$

For our purposes, we typically want to set desired values for α , β , and x_c , variables which represent wrist flexion/extension, radial/ulnar deviation, and handle translation from the elbow, respectively. This means that $\alpha(q') = [\alpha, \beta, x_c]^T$. Now we define $\psi(q')$ and $\bar{\psi}(q', q^*)$ as shown below. Importantly, q^* in Eq. 9 is the vector of the three independent variables assigned the specific values of interest. We additionally define the partial derivative of ψ as $\psi_{q'} \triangleq \frac{\partial \psi(q')}{\partial q'} \in \mathbb{R}^{12 \times 12}$.

$$\psi(q') = \begin{bmatrix} \phi(q') \\ \alpha(q') \end{bmatrix} \in \mathbb{R}^{12 \times 1} \quad (8)$$

$$\bar{\psi}(q', q^*) = \begin{bmatrix} \phi(q') \\ \alpha(q') \end{bmatrix} - \begin{bmatrix} 0 \\ q^* \end{bmatrix} \in \mathbb{R}^{12 \times 1} \quad (9)$$

Lemma II.1 from [2] states that for a set of desired independent values q^* (while not in a singular configuration) where $\bar{\psi}(q', q^*) = 0$ —meaning the constraints are met. This means that for any q^* there exists a unique q' such that

$$q' = \sigma(q^*) \in \mathbb{R}^{3 \times 1} \quad (10)$$

Further,

$$\dot{q}' = \rho^*(q') \dot{q}^* \quad (11)$$

where

$$\rho^*(q') = \psi_{q'}^{-1}(q') \begin{bmatrix} 0_{(9 \times 3)} \\ I_{(3 \times 3)} \end{bmatrix} \in \mathbb{R}^{3 \times 12} \quad (12)$$

A numerical iterative algorithm such as the Newton-Raphson method can be used to find the solution $q' = \sigma(q^*)$. To use Newton-Raphson, first we initialize a vector of our variables q'_0 . Then, a step is taken along the gradient in the direction of the zero of the function until $\bar{\psi}$ is acceptably close to 0.

$$q'_k = q'_{k-1} - \bar{\psi}_{q'}(q'_{k-1})^{-1} \bar{\psi}(q'_{k-1}) \quad (13)$$

The expression for $\rho^*(q')$ is derived from the previous constraint equations:

$$\begin{bmatrix} \phi(q') \\ \alpha(q') \end{bmatrix} = \begin{bmatrix} 0 \\ q^* \end{bmatrix} \quad (14)$$

We then take the time derivative:

$$\frac{d}{dt} \begin{bmatrix} \phi(q') \\ \alpha(q') \end{bmatrix} = \frac{d}{dt} \begin{bmatrix} 0 \\ q^* \end{bmatrix} \quad (15)$$

$$\psi_{q'}(q')\dot{q}' = \begin{bmatrix} 0_{9 \times 3} \\ I_{3 \times 3} \end{bmatrix} \dot{q} \rightarrow \rho^*(q') = \psi_{q'}^{-1} \begin{bmatrix} 0_{9 \times 3} \\ I_{3 \times 3} \end{bmatrix} \quad (16)$$

yielding an expression for $\rho^*(q')$.

Finally, the transformation matrix ${}_{14}^{13}T$ represents the positioning of the handle. The handle translation is represented by the general coordinate q_{18} along the \vec{x}_{13} axis. Dimension a_9 represents the distance between O_{13} and O_{14} in the \vec{y}_{13} direction, and dimension a_{10} is an offset added to q_{18} in the \vec{x}_{13} direction to reach the handle position at O_{14} .

$${}_{14}^{13}T = \begin{bmatrix} 1 & 0 & 0 & a_{10} + q_{18} \\ 0 & 1 & 0 & -a_9 \\ 0 & 0 & 1 & 0 \\ 0 & 0 & 0 & 1 \end{bmatrix}$$

2.3 Full Serial Representation

At times, it is useful and/or necessary to describe the parallel mechanism with serial joint coordinates. This is the case for the robot to be modeled in OpenSim. Therefore, a serial representation of the distal part of the device is described here, where two serial kinematic chains describe the paths to the ends of two of the linear rails and one serial kinematic chain describes the path from the top linear rail, through the spherical joint, to the wrist ring and handle.

Continuing from the end of the proximal section, Frame 5, at the forearm wring, the transformation matrix ${}_{6}^5T$ represents the rotation of the linear slider 1 relative to the forearm ring about the \vec{z}_6 axis. Frame 6 is rotated by the fixed parameter α_5 about \vec{x}_5 , translated by the forearm ring radius R along the \vec{y} direction after this rotation, and then translated by a_5 along \vec{z}_6 .

$${}_{6}^5T = \begin{bmatrix} c_9 & -s_9 & 0 & 0 \\ c\alpha_5 s_9 & c\alpha_5 c_9 & -s\alpha_5 & Rc\alpha_5 - a_5 s\alpha_5 \\ s\alpha_5 s_9 & s\alpha_5 c_9 & c\alpha_5 & Rs\alpha_5 + a_5 c\alpha_5 \\ 0 & 0 & 0 & 1 \end{bmatrix}$$

The transformation matrices ${}_{7}^5T$ and ${}_{8}^5T$ represent the rotation of linear sliders 2 and 3 relative to the forearm ring about their respective \vec{z} axes. Their function is identical to that of ${}_{6}^5T$, with the only difference being the initial rotation of α' and α'' instead of α . These angles space the three frames equally around the forearm ring.

$${}_{7}^5T = \begin{bmatrix} c_{10} & -s_{10} & 0 & 0 \\ c\alpha'_5 s_{10} & c\alpha'_5 c_{10} & -s\alpha'_5 & Rc\alpha'_5 - a_5 s\alpha'_5 \\ s\alpha'_5 s_{10} & s\alpha'_5 c_{10} & c\alpha'_5 & Rs\alpha'_5 + a_5 c\alpha'_5 \\ 0 & 0 & 0 & 1 \end{bmatrix}$$

$${}^5_8T = \begin{bmatrix} c_{11} & -s_{11} & 0 & 0 \\ c\alpha''_5 s_{11} & c\alpha''_5 c_{11} & -s\alpha''_5 & Rc\alpha''_5 - a_5 s\alpha''_5 \\ s\alpha''_5 s_{11} & s\alpha''_5 c_{11} & c\alpha''_5 & Rs\alpha''_5 + a_5 c\alpha''_5 \\ 0 & 0 & 0 & 1 \end{bmatrix}$$

The transformation matrix 6_9T represents the translation of linear rail 1 relative to linear slider in the \vec{x}_6 direction, where the origin of Frame 9 has been translated by a_6 in the $-\vec{z}_6$ direction. Similarly, transformation matrices ${}^7_{10}T$ and ${}^8_{11}T$ represent the translation of linear rails 2 and 3 relative to linear sliders 2 and 3 respectively, with the same translation by a_6 in their frame's $-\vec{z}$ direction.

$${}^6_9T = \begin{bmatrix} 0 & 0 & 0 & q_{12} \\ 0 & 1 & 0 & 0 \\ 0 & 0 & 1 & -a_6 \\ 0 & 0 & 0 & 1 \end{bmatrix}$$

$${}^7_{10}T = \begin{bmatrix} 0 & 0 & 0 & q_{13} \\ 0 & 1 & 0 & 0 \\ 0 & 0 & 1 & -a_6 \\ 0 & 0 & 0 & 1 \end{bmatrix}$$

$${}^8_{11}T = \begin{bmatrix} 0 & 0 & 0 & q_{14} \\ 0 & 1 & 0 & 0 \\ 0 & 0 & 1 & -a_6 \\ 0 & 0 & 0 & 1 \end{bmatrix}$$

The remaining transforms handle the serial chain from linear rail 1 to the wrist ring and handle. Thus, this serial representation does not describe all three of the paths from the forearm ring to the handle, but instead, it covers what is necessary to fully specify the position and orientation of the entire exoskeleton assembly.

The transformation matrix ${}^9_{12}T$ represents the 3-D rotation of the wrist ring relative to linear rail 1 about the center of the spherical bearing connecting them. The relative orientation of the ring is described in terms of X-Y-Z Euler angles as successive rotations, meaning their order of multiplication is left to right. Therefore, the rotational part of this transformation can be composed as

$${}^9_{12}R = R_X(q_{15})R_Y(q_{16})R_Z(q_{17}).$$

However, the rotation matrix ${}^5_{13}R$ is already given by the coordinates defined in the parallel representation: α , β , and γ :

$${}^5_{13}R = R_Y(\alpha)R_Z(\beta)R_X(\gamma).$$

Working backward, the rotation matrix ${}^{12}_{13}R$ accounts for the difference in orientation between the handle and the triangle constructed by connecting the spherical bearings B_i (Figure 3).

$${}^{12}_{13}R = R_Z(\alpha_{12})R_X(-\alpha_{13}).$$

Taking the rotational part of the transformation matrix ${}^5_9T = {}^5_6T {}^6_9T$,

$${}^5_9R = R_X(\alpha_5)R_Z(q_9),$$

we can solve for the rotation matrix ${}^9_{12}R$ in terms of known quantities:

$${}^9_{12}R = {}^5_9R^T {}^5_{13}R {}^{12}_{13}R^T.$$

The three Euler angles q_{15} , q_{16} , and q_{17} can be found from the elements of this matrix as follows:

$$\begin{aligned} q_{15} &= \text{atan2}(-r(2, 3), r(3, 3)) \\ q_{16} &= \text{atan2}(r(1, 3), \sqrt{1 - r^2(1, 3)}) \\ q_{17} &= \text{atan2}(-r(1, 2), r(1, 1)), \end{aligned}$$

where $r(i, j)$ is the element of ${}^9_{12}R$ in the i th row and the j th column.

The transformation matrix ${}^9_{12}T$ is a pure 3-dimensional rotation corresponding to the spherical bearing at B_1 .

$${}^9_{12}T = \begin{bmatrix} c_{16}c_{17} & -c_{16}s_{17} & s_{16} & 0 \\ c_{15}s_{17} + c_{17}s_{15}s_{16} & c_{15}c_{17} - s_{15}s_{16}s_{17} & -c_{16}s_{15} & 0 \\ s_{15}s_{17} - c_{15}c_{17}s_{16} & c_{17}s_{15} + c_{15}s_{16}s_{17} & c_{15}c_{16} & 0 \\ 0 & 0 & 0 & 1 \end{bmatrix}$$

The transformation matrix ${}^{12}_{13}T$ is a fixed transformation (containing no generalized coordinates q_i), that relates the position and orientation of Frame 12 to Frame 13, and is introduced to keep the transformation matrices from becoming overly complicated.

$${}^{12}_{13}T = \begin{bmatrix} c\alpha_{12} & -s\alpha_{12}c\alpha_{13} & -s\alpha_{12}s\alpha_{13} & a_7 \\ s\alpha_{12} & c\alpha_{12}c\alpha_{13} & c\alpha_{12}s\alpha_{13} & -a_8 \\ 0 & -s\alpha_{13} & c\alpha_{13} & 0 \\ 0 & 0 & 0 & 1 \end{bmatrix}$$

Finally, as presented in the previous subsection, the transformation matrix, ${}^{13}_{14}T$, represents the positioning of the handle. The handle translation is represented by the general coordinate q_{18} along the \vec{x}_{13} axis. Dimension a_9 represents the distance between O_{13} and O_{14} in the \vec{y}_{13} direction, and dimension a_{10} is an offset added to q_{18} in the \vec{x}_{13} direction to reach the handle position at O_{14} .

$${}^{13}_{14}T = \begin{bmatrix} 1 & 0 & 0 & a_{10} + q_{18} \\ 0 & 1 & 0 & -a_9 \\ 0 & 0 & 1 & 0 \\ 0 & 0 & 0 & 1 \end{bmatrix}$$

The full list of generalized coordinates and their definitions in the serial representation is shown in Table 6, and the definitions of the coordinate frames are listed in Table 7.

Table 6: Generalized Coordinate Assignment

| Gen. Coord. | Description |
|-------------|------------------------------------|
| q_1 | cart rotation about world y |
| q_2 | cart translation in world x |
| q_3 | cart translation in world y |
| q_4 | cart translation in world z |
| q_5 | exo shoulder abduction |
| q_6 | exo elbow flexion |
| q_7 | counterweight translation |
| q_8 | exo forearm pronation |
| q_9 | (θ_1) exo slider 1 rotation |
| q_{10} | (θ_2) exo slider 2 rotation |
| q_{11} | (θ_3) exo slider 3 rotation |
| q_{12} | (l_1) exo rail 1 translation |
| q_{13} | (l_2) exo rail 2 translation |
| q_{14} | (l_3) exo rail 3 translation |
| q_{15} | exo spherical bearing 1 roll |
| q_{16} | exo spherical bearing 1 yaw |
| q_{17} | exo spherical bearing 1 pitch |
| q_{18} | exo handle position |

3 Statics

3.1 Distal RPS Mechanism

External virtual work done by a closed kinematic chain is defined by

$$\delta w = -(\tau')^\top \dot{q}' \quad (17)$$

where τ' is the n' -by-1 generalized external torque vector for a system described by n' generalized coordinates with n^* degrees of freedom and $n' - n^*$ constraints. Under static equilibrium, $\delta w = 0$.

So, choosing $n^* = 3$ and $n' = 12$ for the MAHI Exo-II, we denote the independent generalized coordinates with a star (*) and the dependent generalized coordinates with a bar (-). The generalized torques are denoted to match the corresponding generalized coordinates, though for the torques, τ^* is now dependent on $\bar{\tau}$.

$$\begin{aligned} q^* &\in \mathbb{R}^3, & q' &\in \mathbb{R}^{12}, & \bar{q} &= q' \setminus q^* \in \mathbb{R}^9 \\ \tau^* &\in \mathbb{R}^3, & \tau' &\in \mathbb{R}^{12}, & \bar{\tau} &= \tau' \setminus \tau^* \in \mathbb{R}^9, \end{aligned}$$

using set notation.

Table 7: Coordinate Frame Descriptions

| Frame | Description |
|-------|--|
| 0 | world frame aligned with the human torso |
| 1 | base of the robot support linear bearing |
| 2 | exo base block |
| 3 | exo upper arm |
| 4 | exo forearm |
| 4' | counterweight |
| 5 | exo wrist base |
| 6 | exo wrist slider 1 |
| 7 | exo wrist slider 2 |
| 8 | exo wrist slider 3 |
| 9 | exo wrist rail 1 |
| 10 | exo wrist rail 2 |
| 11 | exo wrist rail 3 |
| 12 | exo spherical bearing housing 1 |
| 13 | exo wrist ring |
| 14 | exo handle |

The generalized virtual displacements and torques in Eq. 17 can be separated into these subsets. Under static conditions:

$$-(\tau^*)^\top \delta q^* - (\bar{\tau})^\top \delta \bar{q} = 0. \quad (18)$$

Making use of the previously defined mapping $\rho(\cdot)$ between the independent and dependent coordinate velocities (Section 2), where the notation of $\rho(\cdot)$ (and its dimensions) has once again changed to be consistent with this section and *not* the previous kinematics section:

$$\dot{q}' = \rho^*(q') \dot{q}^*, \quad \dot{\bar{q}} = \rho(q') \dot{q}^*, \quad \dot{q}' = \dot{\bar{q}} \cup \dot{q}^*. \quad (19)$$

We use this relationship as a substitution in Eq. 18:

$$[(\tau^*)^\top - (\bar{\tau})^\top \rho(q')] \delta q^* = 0 \quad (20)$$

In order to drop the δq^* and say $(\tau^*)^\top - (\bar{\tau})^\top \rho(q') = 0$, the virtual displacements δq^* must be independent. For the RPS mechanism, we know only $n = 3$ of the coordinates can be independent. Therefore, we can say that $\tau^* = \rho(q')^\top \bar{\tau}$ only for $n = 3$ torques in τ^* . The remaining $n' - n = 9$ torques in $\bar{\tau}$ *must* be specified, but *can* be independent of each other. If they are not defined, then they must be assumed to be zero in order to have a valid solution for the 3 dependent torques τ^* .

The established relationships between joint velocities and torques in the RPS parallel mechanism

can be summarized as follows:

$$\begin{aligned}
q^* &\in \mathbb{R}^3, & q' &\in \mathbb{R}^{12}, & \bar{q} &= q' \setminus q^* \in \mathbb{R}^9 \\
\tau^* &\in \mathbb{R}^3, & \tau' &\in \mathbb{R}^{12}, & \bar{\tau} &= \tau' \setminus \tau^* \in \mathbb{R}^9 \\
\dot{q}' &= \rho^*(q') \dot{q}^*, & \dot{\bar{q}} &= \rho(q') \dot{q}^*, & \dot{q}' &= \dot{\bar{q}} \cup \dot{q}^* \\
\tau' &= \bar{\rho}^\top(q') \bar{\tau}, & \tau^* &= \rho^\top(q') \bar{\tau}, & \tau' &= \bar{\tau} \cup \tau^*
\end{aligned}$$

3.2 Proximal Serial Joints

4 Dynamics

Determination of the full equations of motion for the MAHI Exo-II is beyond the scope of this text; however, the exact equations can be found computationally given the information provided in the kinematics and statics sections, along with the inertial properties of the rigid bodies composing the robot. More information on the dynamics of parallel mechanisms can also be found in [2].

For each of the coordinate frames associated with moving rigid bodies of the robot (including bodies that are locked in place during normal operation), we have calculated the theoretical mass, location of center of mass, and elements of the inertia tensor using an accurate SolidWorks model that includes all known properties, as well as all fasteners and other peripheral parts present that would affect inertial properties. All values are given with a precision of 8 digits after the decimal point, in standard SI units. Mass is given in kg. Position of the center of mass in m is expressed in the moving body frame. The elements of the inertia tensor (kg m^2) are arranged in a symmetric two-dimensional matrix, calculated at the center of mass and oriented in the moving body frame.

Frame 3, Exo Upper Arm:

$$\begin{aligned}
m_3 &= 3.42222721, & {}^3\vec{P}_{3,COM} &= \begin{bmatrix} 0.04238470 \\ -0.07466000 \\ -0.00583083 \end{bmatrix} \\
{}^3I_3 &= \begin{bmatrix} 0.03278369 & -0.00882058 & -0.00039780 \\ -0.00882058 & 0.02600980 & 0.00135900 \\ -0.00039780 & 0.00135900 & 0.04034464 \end{bmatrix}
\end{aligned}$$

Frame 4, Exo Forearm:

$$\begin{aligned}
m_4 &= 1.75487178, & {}^4\vec{P}_{4,COM} &= \begin{bmatrix} 0.05408420 \\ -0.03777320 \\ 0.00297689 \end{bmatrix} \\
{}^4I_4 &= \begin{bmatrix} 0.01371556 & -0.00398585 & -0.00095332 \\ -0.00398585 & 0.02047318 & 0.00071175 \\ -0.00095332 & 0.00071175 & 0.01731919 \end{bmatrix}
\end{aligned}$$

Frame 4', Exo Counterweight:

$$m_{4'} = 5.35239000, \quad {}^4\vec{P}_{4',COM} = \begin{bmatrix} 0 \\ 0 \\ 0 \end{bmatrix}$$

$${}^4I_{4'} = \begin{bmatrix} 0.00700388 & 0 & 0 \\ 0 & 0.00700388 & 0 \\ 0 & 0 & 0.01317901 \end{bmatrix}$$

Frame 5, Exo Wrist Base:

$$m_5 = 1.45613142, \quad {}^5\vec{P}_{5,COM} = \begin{bmatrix} -0.00401306 \\ -0.00116828 \\ -0.00011279 \end{bmatrix}$$

$${}^5I_5 = \begin{bmatrix} 0.01747099 & 0.00006494 & 0.00000848 \\ 0.00006494 & 0.00904374 & -0.00000851 \\ 0.00000848 & -0.00000851 & 0.00895693 \end{bmatrix}$$

Frame 6, Exo Wrist Slider 1:

$$m_6 = 0.05994136, \quad {}^6\vec{P}_{6,COM} = \begin{bmatrix} 0 \\ 0 \\ -0.00868910 \end{bmatrix}$$

$${}^6I_6 = \begin{bmatrix} 0.00000961 & 0 & 0 \\ 0 & 0.00000989 & 0 \\ 0 & 0 & 0.00000890 \end{bmatrix}$$

Frame 7, Exo Wrist Slider 2:

$$m_7 = 0.05994136, \quad {}^7\vec{P}_{7,COM} = \begin{bmatrix} 0 \\ 0 \\ -0.00868910 \end{bmatrix}$$

$${}^7I_7 = \begin{bmatrix} 0.00000961 & 0 & 0 \\ 0 & 0.00000989 & 0 \\ 0 & 0 & 0.00000890 \end{bmatrix}$$

Frame 8, Exo Wrist Slider 3:

$$m_8 = 0.05994136, \quad {}^8\vec{P}_{8,COM} = \begin{bmatrix} 0 \\ 0 \\ -0.00868910 \end{bmatrix}$$

$${}^8I_8 = \begin{bmatrix} 0.00000961 & 0 & 0 \\ 0 & 0.00000989 & 0 \\ 0 & 0 & 0.00000890 \end{bmatrix}$$

Frame 9, Exo Wrist Rail 1:

$$m_9 = 0.14820004, \quad {}^9\vec{P}_{9,COM} = \begin{bmatrix} -0.08803880 \\ 0.00000222 \\ 0.00949584 \end{bmatrix}$$

$${}^9I_9 = \begin{bmatrix} 0.00002001 & -0.00000005 & -0.00012515 \\ -0.00000005 & 0.00146169 & 0 \\ -0.00012515 & 0 & 0.00144578 \end{bmatrix}$$

Frame 10, Exo Wrist Rail 2:

$$m_{10} = 0.14820004, \quad {}^{10}\vec{P}_{10,COM} = \begin{bmatrix} -0.08803880 \\ 0.00000222 \\ 0.00949584 \end{bmatrix}$$

$${}^{10}I_{10} = \begin{bmatrix} 0.00002001 & -0.00000005 & -0.00012515 \\ -0.00000005 & 0.00146169 & 0 \\ -0.00012515 & 0 & 0.00144578 \end{bmatrix}$$

Frame 11, Exo Wrist Rail 3:

$$m_{11} = 0.14820004, \quad {}^{11}\vec{P}_{11,COM} = \begin{bmatrix} -0.08803880 \\ 0.00000222 \\ 0.00949584 \end{bmatrix}$$

$${}^{11}I_{11} = \begin{bmatrix} 0.00002001 & -0.00000005 & -0.00012515 \\ -0.00000005 & 0.00146169 & 0 \\ -0.00012515 & 0 & 0.00144578 \end{bmatrix}$$

| ij | $a(ij)$ | μ_{ij} | σ_{ij} | γ_{ij} | b_{ij} | α_{ij} | d_{ij} | θ_{ij} | r_{ij} |
|--------|---------|------------|---------------|---------------|----------|---------------|----------|------------------|----------|
| 11 (1) | 0 (0) | 1 | 0 | 0 | 0 | 0 | 0 | q_1 | 0 |
| 21 (2) | 1 (1) | 1 | 0 | 0 | 0 | $\pi/2$ | 0 | $q_2 + \alpha_5$ | a_4 |
| 31 (3) | 21 (2) | 0 | 0 | 0 | 0 | $-\pi/2$ | R | q_{31} | a_{56} |
| 32 (4) | 31 (3) | 1 | 1 | 0 | 0 | $\pi/2$ | 0 | 0 | q_{32} |
| 41 (5) | 21 (2) | 0 | 0 | $2\pi/3$ | 0 | $-\pi/2$ | R | q_{41} | a_{56} |
| 42 (6) | 41 (5) | 1 | 1 | 0 | 0 | $\pi/2$ | 0 | 0 | q_{42} |
| 51 (7) | 21 (2) | 0 | 0 | $4\pi/3$ | 0 | $-\pi/2$ | R | q_{51} | a_{56} |
| 52 (8) | 51 (7) | 1 | 1 | 0 | 0 | $\pi/2$ | 0 | 0 | q_{52} |

Table 8: Caption

Frame 13, Exo Wrist Ring:

$$m_{13} = 0.20360330, \quad {}^{13}\vec{P}_{13,COM} = \begin{bmatrix} 0.04604890 \\ -0.05986810 \\ -0.00647995 \end{bmatrix}$$

$${}^{13}I_{13} = \begin{bmatrix} 0.00108391 & -0.00064377 & -0.00000844 \\ -0.00064377 & 0.00082063 & 0.00002664 \\ -0.00000844 & 0.00002664 & 0.00158304 \end{bmatrix}$$

Frame 14, Exo Handle:

$$m_{14} = 0.16125801, \quad {}^1P_{14,COM} = \begin{bmatrix} 0 \\ 0.06844240 \\ 0 \end{bmatrix}$$

$${}^1I_{14} = \begin{bmatrix} 0.00103949 & 0 & 0 \\ 0 & 0.00002597 & 0 \\ 0 & 0 & 0.00103949 \end{bmatrix}$$

Modified DH Parameters for parallel mechanism

$\mu_j = 1$ if joint is active

$\mu_j = 0$ if joint is passive

$\sigma_i = 0$ if joint i is a R joint

$\sigma_i = 1$ if joint i is a P joint

$\bar{\sigma}_i = 1 - \sigma_i$

References

- [1] J. A. French, C. G. Rose, and M. K. O'malley. System characterization of mahi exo-ii: a robotic exoskeleton for upper extremity rehabilitation. In *Proceedings of the ASME Dynamic Systems and Control Conference. ASME Dynamic Systems and Control Conference*, volume 2014. NIH Public Access, 2014.
- [2] F. H. Ghorbel, O. Chetelat, R. Gunawardana, and R. Longchamp. Modeling and set point control of closed-chain mechanisms: theory and experiment. *IEEE Transactions on Control Systems Technology*, 8(5):801–815, Sep. 2000.
- [3] A. Gupta and M. K. O'Malley. Design of a haptic arm exoskeleton for training and rehabilitation. *IEEE/ASME Transactions on mechatronics*, 11(3):280–289, 2006.
- [4] A. Gupta, M. K. O'Malley, V. Patoglu, and C. Bugar. Design, control and performance of ricewrist: a force feedback wrist exoskeleton for rehabilitation and training. *The International Journal of Robotics Research*, 27(2):233–251, 2008.
- [5] M. K. O'Malley, A. Sledd, A. Gupta, V. Patoglu, J. Huegel, and C. Bugar. The ricewrist: A distal upper extremity rehabilitation robot for stroke therapy. In *ASME 2006 International Mechanical Engineering Congress and Exposition*, pages 1437–1446. American Society of Mechanical Engineers Digital Collection, 2006.
- [6] A. U. Pehlivan, O. Celik, and M. K. O'Malley. Mechanical design of a distal arm exoskeleton for stroke and spinal cord injury rehabilitation. In *2011 IEEE International Conference on Rehabilitation Robotics*, pages 1–5. IEEE, 2011.